Composites Research

Vol. 31, No. 2, 76-81 (2018)
DOI: http://dx.doi.org/10.7234/composres.2018.31.2.076
ISSN 2288-2103(Print), ISSN 2288-2111(Online)

Paper

Role of Electron Acceptor-donor on Elemental Mercury Removal Using Nano-silver-plated Activated Carbons Complexes

Hyo In Lee*, Yoon-Ji Yim*, Kyong-Min Bae*, Soo-Jin Park*†

ABSTRACT: In this study, the elemental mercury removal behaviors of silver-plated porous carbons materials were investigated. The pore structures and total pore volumes of the hybrid materials were analyzed by N_2 adsorption/desorption analysis at 77 K. The pore structures and surface morphologies of the hybrid materials were characterized by XRD and SEM, respectively. The elemental mercury adsorption capacities of all silver-plated porous carbons hybrid materials were higher than those of the as-received samples, despite the fact that the specific surface areas and total pore volumes decreased with increasing metal loading time. It was found that silver nanoparticles showed excellent elemental mercury removal behaviors in carbonaceous hybrid materials.

Key Words: Elemental mercury removal, Silver-plated carbonaceous materials, Porous carbons, Textural properties

1. INTRODUCTION

Mercury is a major toxic metal and an important source of air pollution—addressed in the 1990 Clean Air Act Amendments (CAAA)—due to its volatility, persistence, bioaccumulation in the environment, and impact on neurological health. Although mercury is one of the least abundant trace metals in coal, the volume of coal consumed globally is now over 5 billion ton per year and increasing (China □2.7 billion ton, United States □1.7 billion ton, and India □0.5 billion ton). Coal-fired utility boilers are recognized as the dominant anthropogenic source of mercury. As a result, attempts to establish a fundamental understanding of the behavior of mercury in coal-fired power plants and to explore cost-effective methods for removing mercury from flue gases have received increasing attention over the past decade [1-4]. Mercury is carcinogenic, mutagenic, and teratogenic, and promotes tyrosinemia. A high concentration of mercury causes impairment of pulmonary and kidney function, chest pain, and dyspnea. Several important ecological accidents caused by mercury—notably between 1953 and 1956 in Minamata's bay in Japan—are known.

The adsorption process of mercury in coal-fired flue gas is complicated. A number of studies have been carried out to understand the mercury adsorbing mechanism of activated carbons (ACs) [5-7]. For example, sulfur trioxide was recently found to have a strong inhibitory effect on Hg^0 adsorption [5]. In the presence of NO_2, Hg^0 was catalytically oxidized on the surface to generate nonvolatile nitrate $Hg(NO_3)_2$, which was attached to basic sites on the carbon. Adsorption of Hg^0 by ACs is determined by many factors such as ACs surface characteristics, temperature, and composition of the flow gas.

Numerous physical and chemical separation processes such as solvent extraction, ion-exchange, precipitation, membrane separation, reverse osmosis, coagulation, and photoreduction have been applied for the effective reduction of mercury concentrations from aqueous solutions. Normally, activity depends on the nature of the support, which may modify the properties of the active phase. Both physical and chemical properties of the support—its acidity, reducibility, and the extent of interaction with the active metal—play important roles in the complex chemistry of supported metal catalysts [8-12].

The objective of this study is to prepare silver-plated porous carbons hybrid materials by a known plating technique and to evaluate the efficiency of elemental mercury removal as a function of the plated silver contents. Silver is known to have a

Received 22 February 2018, received in revised form 26 April 2018, accepted 29 April 2018

*Department of Chemistry, Inha University
*†Department of Chemistry, Inha University, Corresponding author (E-mail: sjpark@inha.ac.kr)

negative charge in aqueous solutions opposite to that of elemental mercury, and this property improve the ability to remove elemental mercury by electrical adsorption [22]. The mercury removal ability in enhanced by the combination of physical adsorption of activated carbons utilizing the large specific surface area and electrical adsorption of silver.

2. EXPERIMENTAL

2.1 Sample preparation

Porous carbons (PCs) were supplied by Hanil Green Tech of Korea. The silver-plated PCs procedure used here is identical to that in a previous study [13,14]. Before deposition, PCs were immersed in 10 wt% nitric acid for 30 min at room temperature (to remove impurities) and rinsed with distilled water. The purified PCs were then sequentially activated in tin chloride ($SnCl_2$) and a palladium chloride ($PdCl_2$) solution. Sn^{2+} ions were initially deposited on the surfaces of the PCs and increases the reactivity of the next step. Pd^{2+} ions were reduced to Pd^0 by Sn^{2+} to form catalytic centers that silver can react and be reduced. Silver-plated PCs were obtained by immersing the palladium-loaded PCs in a silver plating bath for 5, 10, and 25 min. The silver-plated PCs are named Ag-PCs-t and t is plating time (5, 10, and 25 min). Conditions of the silver plating bath was shown in Table 1. The pH of the silver plating solution was adjusted to about 5.0 and the temperature was 90°C and a schematic explanation of the preparation process is shown in Fig. 1.

2.2 Surface characterization

The silver content was characterized by atomic absorption spectrophotometry (AAS). To study the surface structures of the Ag-PCs, X-ray diffraction (XRD) patterns were characterized with a Rigaku model MAX 2200v diffraction meter (Cu-Kα).

XRD patterns were obtained in the 2θ range between 20° and 80° at a scanning rate of 0.2° s^{-1}. Scanning electron microscopy (SEM, S-4200, Hitachi, Japan) was used to observe the surface morphologies of the Ag-PCs. An energy-dispersive X-ray spectroscope (EDS, AN-10000/85S, LINK system, Japan) was used to evaluate the silver contents in the Ag-PCs.

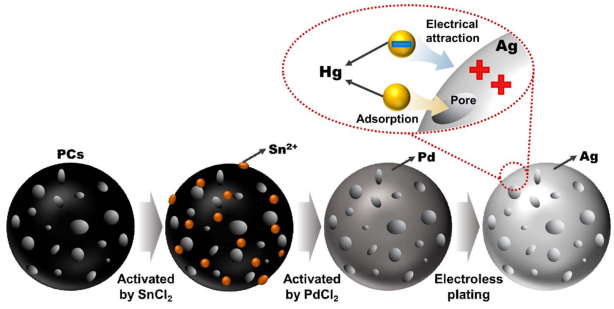

Fig. 1. Schematic illustration of Ag-PCs preparation process by electroless plating method and removal process of elemental mercury by silver-plated PCs

Table 1. Composition of the silver plating bath

Compositions	AgCN	5 g/L
	Na_2CO_3	3 g/L
	NaCN	12 g/L

2.3 Textural properties

N_2 adsorption isotherms were obtained using a Belsorp Max (BEL, Japan) at 77 K. The specimens were degassed at 573 K for 10 h to a residual pressure of lower than 10^{-6} Torr. The amount of N_2 adsorbed on a specimen was used to calculate the specific surface area through the Brunauer-Emmett-Teller (BET) equation [15]. The micropore volume was calculated using the Dubinin-Radushkevitch (D-R) equation [16]:

$$\log(W) = \log(W_0) + M(\log^2(P_0/P)) \quad (1)$$

where W is the amount of adsorbate adsorbed at equilibrium, W_0 the micropore volume calculated from the intercept of the $\log(W) - \log^2(P_0/P)$ plot, and M is the slope of the best-fit line.

2.4 Elemental mercury removal efficiency Textural properties

Experiments were performed using a lab-scale apparatus. Using this apparatus, a gas stream with the required temperature and elemental mercury concentration was produced, and the capture of elemental mercury on a fixed bed of adsorbent material was performed. The 12.7 mm diameter quartz reactor was placed inside a temperature-controllable tubular furnace. For each experiment, 1.0 g of sample was loaded and packed inside a quartz tube. A carrier gas was fed into the adsorption apparatus at a flow rate of 100 mL min^{-1}. Elemental mercury gas was generated using elemental mercury permeation tubes (Dynacalibrator® Model 150, VICI Metronics Inc., USA) and the concentration of elemental mercury gas was maintained at 800 μg m^{-3} during the experimental process. The inlet and outlet concentrations of elemental mercury were measured using a mercury analyzer (VM-3000, Mercury Instruments, Germany). Sulfur was used to capture elemental mercury from the effluent gas.

3. RESULTS AND DISCUSSION

3.1 Surface morphology analysis

Fig. 2(a) shows the silver content of the Ag-PCs studied as a function of the treatment time. The correlation coefficient for metal contents with deposition time was 0.992 (R^2), indicating that the silver contents of the Ag-PCs was proportional to the plating time. Fig. 2(b) shows the EDS result of the Ag-PCs-10 sample. Carbon, oxygen, and silver were detected in the Ag-PCs-10 sample. Fig. 2(c) and (d) shows SEM images and image mapping results of the Ag-PCs-10 sample to examine

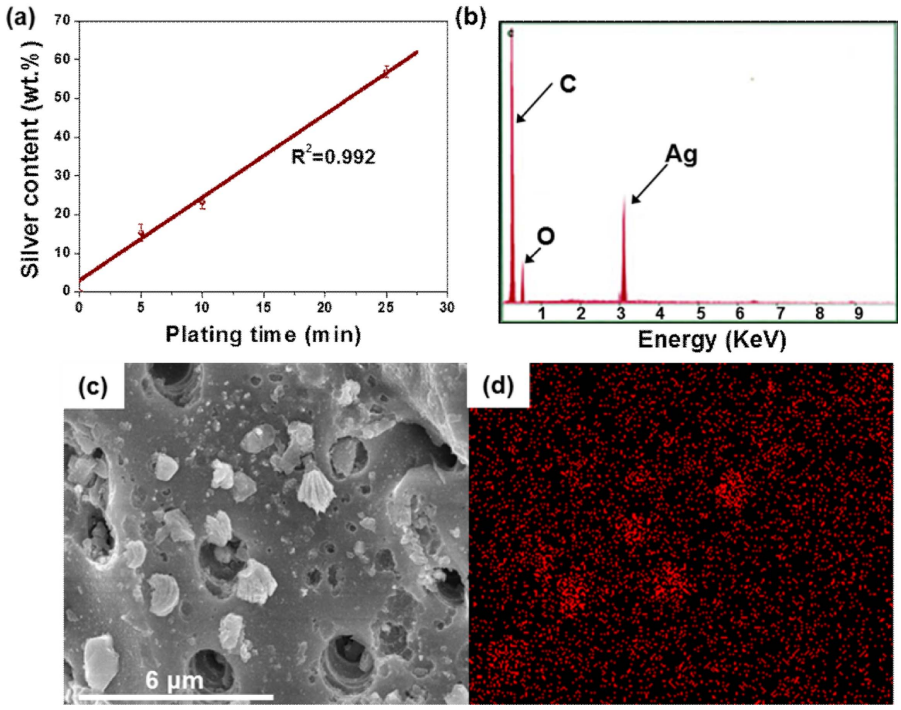

Fig. 2. (a) Silver contents of Ag-PCs as a function of the plating time (R^2 is the correlation coefficient between metal content and plating time). (b) EDS image of the Ag-PCs-10 sample. (c) SEM image of the Ag-PCs-10 sample. (d) Image mapping result of the Ag-PCs-10 sample

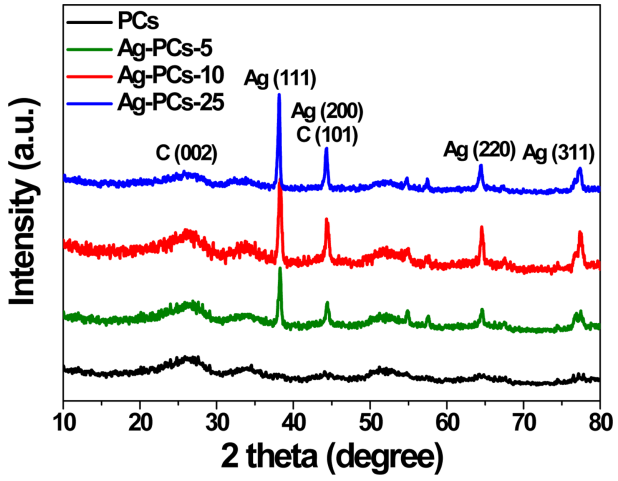

Fig. 3. XRD patterns of Ag-PCs as a function of the plating time

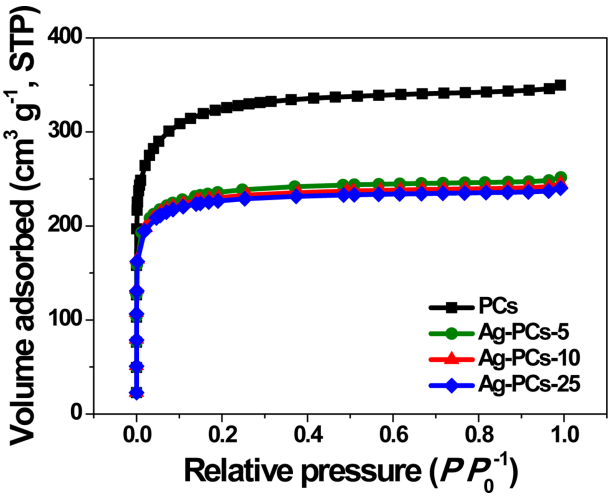

Fig. 4. Adsorption isotherms of N_2/77 K on Ag-PCs as a function of the plating time

the surface morphologies of the Ag-PCs before and after silver plating. The silver particles completely covered the surfaces of Ag-PCs and the silver particles were dispersed well, indicating that micro- and mesopores of the PCs can be blocked due to the metal loading.

An understanding of the surface structure can be achieved by wide-angle XRD. Fig. 3 shows wide-angle XRD diffraction results of the Ag-PCs; the peaks around 2θ = 38°, 44°, 64°, and 77° correspond to the (111), (200), (220), and (311) planes of silver, respectively [17,18]. Intensities of the silver peaks and crystallinities of the Ag-PCs strengthened with increasing plating time.

The N_2 adsorption isotherms of the Ag-PCs are shown in Fig. 4. All of the samples exhibited Type-I isotherms according to the IUPAC classification, having well-developed micropores [19]. Most of the pore volume of the samples was filled below a relative pressure of ~0.1, indicating high microporosity. After the adsorbed volume sharply increased to 0.1 relative pressure, the isotherms showed very small increases of the pore volume

Table 2. Textural properties of the Ag-PCs as a function of the plating time

Samples	[a]S_{BET} (m^2/g)	[b]V_{Total} (cm^3/g)	[c]V_{Micro} (cm^3/g)	[d]D_p (nm)
PCs	1158	0.553	0.476	1.91
Ag-PCs-5	864	0.389	0.343	1.85
Ag-PCs-10	823	0.379	0.337	1.84
Ag-PCs-25	810	0.371	0.333	1.83

[a]Specific surface area
[b]Total pore volume
[c]Micropore volume
[d]Average pore diameter

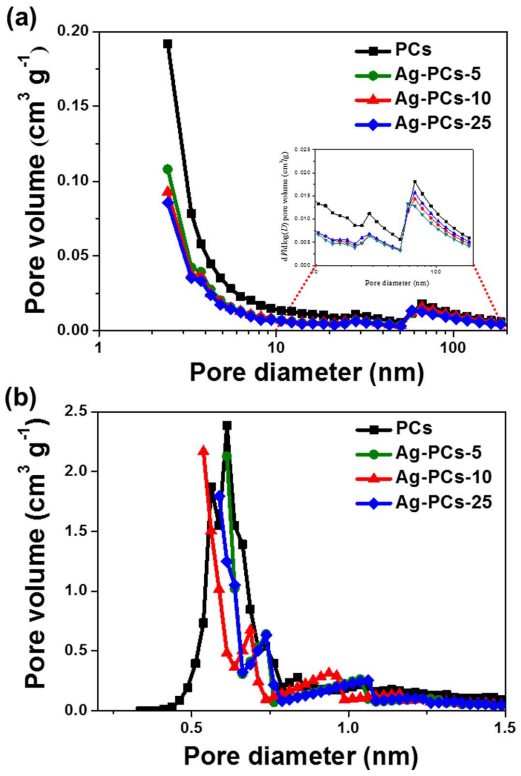

Fig. 5. (a) BJH and (b) HK pore size distributions of Ag-PCs as a function of the plating time

to ~1.0 relative pressure with no further adsorption. This result indicates that silver particles had some influence on the blocking or filling of pores on the PC surfaces.

Table 2 displays the textural properties of the samples as calculated from the N_2/77 K adsorption isotherms. The PCs had specific surface area of 1158 m^2 g^{-1}, total pore volume of 0.553 cm^2 g^{-1}, and micropore volume of 0.476 cm^2 g^{-1}. Ag-PCs exhibited decreasing specific surface area and decreasing total and micropore volumes as the plating time increased. This result indicates that the adsorption capacities of the PCs can be diminished by the silver nanoparticles produced, due to the blocking or filling of the micropores in the PCs.

Fig. 5 displays the BJH and HK pore size distributions of Ag-PCs. Firstly, mesopore peaks of Ag-PCs were observed at around 2.5, 28, and 66 nm. Secondly, the pore size distribution of Ag- PCs decreased relative to the PCs. Thirdly, the pore volumes of Ag-PCs at □76 nm decreased dramatically. As a result, it was found that the micro- and mesopores of PCs can be blocked by plated silver metal.

3.2 Removal efficiency

Fig. 6 shows the removal of elemental mercury by PCs and Ag-PCs as a function of the plating time. All tests were conducted at 423 K for 80 min in the elemental mercury adsorption apparatus (the internal temperature of the apparatus was maintained in the range 418-428 K). As mentioned in the experimental section, the initial concentration of elemental was approximately 800 μg m^{-3} (balanced by N_2 gas). Normally, exhaust mercury concentration is strictly regulated to lower than 100 μg m^{-3}. Therefore, in the present study, outlet concentration >90% (less 10% removal by the filter media) is specified as the breakthrough of the Ag-PCs. The outlet elemental mercury concentration is reported in dimensionless form (Hg_{out}/Hg_{in}) as the ratio between the outlet and inlet elemental mercury concentrations (breakthrough curves).

The PCs showed breakthrough after just 7 min of reaction time, indicating that the PCs could not remove elemental mercury. In contrast, all Ag-PCs showed better removal efficiencies than those of the PCs, with Ag-PCs-10 showing the maximum. The Ag-PCs-10 sample showed breakthrough at 62 min. The removal capacity listed in Table 3 was calculated using the breakthrough time and the equation is represented below:

$$E_{removal} = \frac{C_{Hg} Q t_{total}}{w} \cdot \frac{Hg_{out}}{Hg_{in}} \quad (2)$$

where $E_{removal}$ is the elemental mercury removal efficiency of prepared samples, C_{Hg} is the concentration of elemental mercury gas, Q is the volumetric flow rate, t_{total} is the total flow

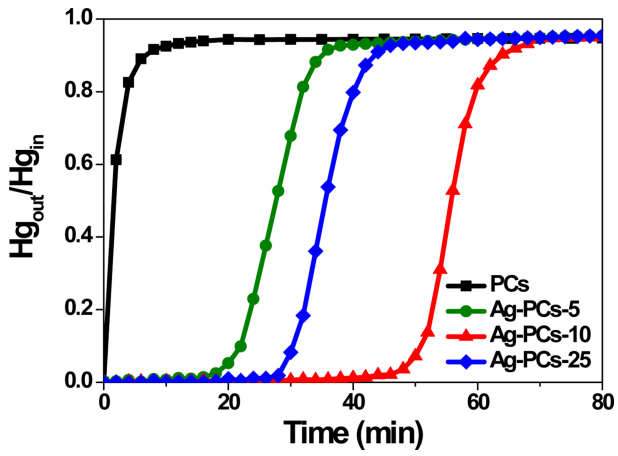

Fig. 6. Breakthrough curves of elemental mercury removal using Ag-PCs as a function of the plating time

Table 3. The breakthrough parameters for elemental mercury removal of Ag-PCs

Samples	Removal capacity (μg g^{-1})
PCs	0.581
Ag-PCs-5	2.640
Ag-PCs-10	4.822
Ag-PCs-25	3.204

time (min), *w* is the weight of loaded samples, and Hg_{out}/Hg_{in} is the breakthrough on points with > 90% removal [20]. The removal efficiency was enhanced with immersing time, although the specific surface area decreased. These results suggest that removal ability strongly depended on silver content and this effect originated from attraction between silver and elemental mercury. It has been reported by many researchers that silver has a positive charge in the elemental state and that elemental mercury has a negative charge [21-24].

Elemental mercury adsorption severely decreased at Ag-PCs-25. This result means that the elemental mercury removal activity of the Ag-PCs depended on the silver contents and on the adsorption characteristics of the samples. In conclusion, the elemental mercury removal efficiencies of the PCs were strongly enhanced by the silver loading, but control of the silver contents and adsorption characteristics is needed to determine the optimal silver contents.

4. CONCLUSIONS

We investigated the elemental mercury adsorption behaviors of Ag-PCs hybrid materials. Based on the experimental results, elemental mercury adsorption of all Ag-PCs occurred at levels higher than those of the PCs. The efficiency increased with increasing plating time up to Ag-PCs-10 and then decreased in Ag-PCs-25 despite Ag-PCs-25 having a higher silver contents than Ag-PCs-10. With increase in plating time, silver metal blocked the pores of PCs and these influenced the adsorption of elemental mercury. However, the major force for the removal of elemental mercury is the electric attraction between silver and mercury. This force affected the mercury removal capacity, which improved as the silver contents increased. In conclusion, when silver plating is accomplished on a range of well-developed micropores, the technique can lead to a useful method for removing elemental mercury on carbon surfaces.

ACKNOWLEDGEMENT

This work was supported by the Korea Institute of Energy Technology Evaluation and Planning (KETEP) and the Ministry of Trade, Industry & Energy (MOTIE) of the Republic of Korea (20153030031710) and Traditional Culture Convergence Research Program through the National Research Foundation of Korea(NRF) funded by the Ministry of Science, ICT & Future Plannig (2016M3C1B5952897).

REFERENCES

1. Darbha, G.K., Singh, A.K., Rai, U.S., Yu, E., Yu, H., and Chandra Ray, P., "Selective Detection of Mercury (II) ion Using Nonlinear Optical Properties of Gold Nanoparticles," *Journal of the American Chemical Society*, Vol. 130, No. 25, 2008, pp. 8038-8043.
2. Issaro, N., Abi-Ghanem, C., and Bermond, A., "Fractionation Studies of Mercury in Soils and Sediments: A Review of the Chemical Reagents Used for Mercury Extraction," *Analytica Chimica Acta*, Vol. 631, No. 1, 2009, pp. 1-12.
3. Pavlish, J.H., Hamre, L.L., and Zhuang, Y., "Mercury Control Technologies for Coal Combustion and Gasification Systems," *Fuel*, Vol. 89, No. 4, 2010, pp. 838-847.
4. ShamsiJazeyi, H., and Kaghazchi, T., "Investigation of Nitric Acid Treatment of Activated Carbon for Enhanced Aqueous Mercury Removal," *Journal of Industrial and Engineering Chemistry*, Vol. 16, No. 5, 2010, pp. 852-858.
5. Bae, K.M., Kim, B.J., and Park, S.J., "A Review of Elemental Mercury Removal Processing," *Carbon letters*, Vol. 12, No. 3, 2011, pp. 121-130.
6. Ghorishi, S.B., Keeney, R.M., Serre, S.D., Gullett, B.K., and Jozewicz, W.S., "Development of a Cl-impregnated Activated Carbon for Entrained-flow Capture of Elemental Mercury," *Environmental Science & Technology*, Vol. 36, No. 20, 2002, pp. 4454-4459.
7. Zeng, H., Jin, F., and Guo, J., "Removal of Elemental Mercury from Coal Combustion Flue Gas by Chloride-impregnated Activated Carbon," *Fuel*, Vol. 83, No. 1, 2004, pp. 143-146.
8. Kim, B.J., and Park, S.J., "Optimization of the Pore Structure of Nickel/graphite Hybrid Materials for Hydrogen Storage," *International Journal of Hydrogen Energy*, Vol. 36, No. 1, 2011, pp. 648-653.
9. Harry, I.D., Saha, B., and Cumming, I.W., "Effect of Electrochemical Oxidation of Activated Carbon Fiber on Competitive and Noncompetitive Sorption of Trace Toxic Metal Ions from Aqueous Solution," *Journal of Colloid and Interface Science*, Vol. 304, No. 1, 2006, pp. 9-20.
10. Miyanaga, S., Hiwara, A., and Yasuda, H., "Preparation and High Bacteriostatic Action of the Activated Carbons Possessing Ultrafine Silver Particles," *Science and Technology of Advanced Materials*, Vol. 3, No. 2, 2002, pp. 103-109.
11. Zhang, S., Fu, R., Wu, D., Xu, W., Ye, Q., and Chen, Z., "Preparation and Characterization of Antibacterial Silver-dispersed Activated Carbon Aerogels," *Carbon*, Vol. 42, No. 15, 2004, pp. 3209-3216.
12. Park, S.J., Seo, M.K., and Rhee, K.Y., "Studies on Mechanical Interfacial Properties of Oxy-fluorinated Carbon Fibers-reinforced Composites," *Materials Science and Engineering: A*, Vol. 356, No. 1, 2003, pp. 219-226.
13. Kim, B.J., and Park, S.J., "Antibacterial Behavior of Transition-metals-decorated Activated Carbon Fibers," *Journal of Colloid*

and Interface Science, Vol. 325, No. 1, 2008, pp. 297-299.
14. Park, S.J., and Jung, W.Y., "Adsorption Behaviors of Chromium (III) and (VI) on Electroless Cu-plated Activated Carbon Fibers," *Journal of Colloid and Interface Science*, Vol. 243, No. 2, 2001, pp. 316-320.
15. Brunauer, S., Emmett, P.H., and Teller, E., "Adsorption of Gases in Multimolecular Layers," *Journal of the American Chemical Society*, Vol. 60, No. 2, 1938, pp. 309-319.
16. Dubinin, M.M., and Plavnik, G.M., "Microporous Structures of Carbonaceous Adsorbents," *Carbon*, Vol. 6, No. 2, 1968, pp. 183-192.
17. Grunwaldt, J.D., Atamny, F., Göbel, U., and Baiker, A., "Preparation of thin Silver Films on Mica Studied by XRD and AFM," *Applied Surface Science*, Vol. 99, No. 4, 1996, pp. 353-359.
18. Park, S.J., and Jang, Y.S., "Preparation and Characterization of Activated Carbon Fibers Supported with Silver Metal for Antibacterial Behavior," *Journal of Colloid and Interface Science*, Vol. 261, No. 2, 2003, pp. 238-243.
19. Bansal, R.C., and Goyal, M., "Activated Carbon Adsorption", CRC Press, New York, 2005.
20. Lakshmipathy, R., and Sarada, N.C., "A Fixed Bed Column Study for the Removal of Pb^{2+} Ions by Watermelon Rind," *Environmental Science: Water Research & Technology*, Vol. 1, No. 2, 2015, pp. 244-250.
21. Zain, N.M., Stapley, A.G.F., and Shama, G., "Green Synthesis of Silver and Copper Nanoparticles Using Ascorbic Acid and Chitosan for Antimicrobial Applications," *Carbohydrate Polymers*, Vol. 112, 2014, pp. 195-202.
22. Mulvaney, P., Linnert, T., and Henglein, A., "Surface Chemistry of Colloidal Silver in Aqueous Solution: Observations on Chemisorption and Reactivity," *The Journal of Physical Chemistry*, Vol. 95, No. 20, 1991, pp. 7843-7846.
23. He, P., Wu, J., Jiang, X., Pan, W., and Ren, J., "Effect of SO_3 on Elemental Mercury Adsorption on a Carbonaceous Surface," *Applied Surface Science*, Vol. 258, No. 22, 2012, pp. 8853-8860.
24. Sun, X., Hwang, J.Y., and Xie, S., "Density Functional Study of Elemental Mercury Adsorption on Surfactants," *Fuel*, Vol. 90, No. 3, 2011, pp. 1061-1068.